Available online at www.sciencedirect.com
SCIENCE DIRECT
International Journal of Heat and Mass Transfer 49 (2006) 640–648
International Journal of HEAT and MASS TRANSFER
www.elsevier.com/locate/ijhmt

Simplified approach of turbulent film condensation on an inclined elliptical tube

Hai-Ping Hu [a,1], Cha'o-Kuang Chen [b,*]

[a] Department of Information Management, Tainan Woman's College of Arts and Technology, 529 Chung Cheng Road, Yung Kang City, Tainan 71002, Taiwan, ROC
[b] Department of Mechanical Engineering, National Cheng Kung University, Tainan 70101, Taiwan, ROC

Received 22 April 2005; received in revised form 18 August 2005
Available online 13 October 2005

Abstract

The present theoretical study investigates turbulent film condensation on an inclined elliptical tube. Adopting the assumption of an isothermal wall surface, the energy equation, forced balance equations and thermal balance equations are derived to describe the phenomena of the condensate film. Results are obtained for the heat transfer coefficient over a wide range of vapor velocities, i.e. low condensation parameter to high condensation parameter. The optimal inclination angle of the tube in different length–radius ratios and eccentricity can be obtained in the present results. This study also discusses the influence of the degree of eccentricity of the elliptical tube on the heat transfer coefficient. Finally, a comparison is provided between the results of the present study and those reported in a previous theoretical study. It is found that a good agreement exists between the two sets of results.

Keywords: Inclined; Turbulent; Condensation; Eccentricity

1. Introduction

Nusselt, who is regarded by many as the pioneering investigator of film condensation, conducted an investigation into laminar film condensation on surfaces of various forms in 1916. Since that time, various other researchers have also studied laminar film condensation of quiescent vapors. For example, Sparrow and Gregg [1] considered the problem of vapor condensation on horizontal cylinders. Meanwhile, Dhir and Lienhard [2] proposed a general integral method, based largely on Nusselt's work, to predict the heat transfer coefficient for the non-circular cross-section condensation problem. Their study focused particularly on the effects of non-uniform gravity.

Shekriladze and Gomelauri [3] investigated the problem of laminar film condensation of flowing vapor and analyzed film condensation on horizontal tubes under low velocity vapor flow conditions. The results indicated that the shearing stress on the friction surface depends on the momentum transferred by the suction mass. A review of the literature shows that various researchers have studied forced convection in laminar film condensation on horizontal tubes. For example, Fujii et al. [4] studied the two-phase boundary layer equations of laminar film condensation on a horizontal cylinder. It was shown that the mean heat transfer coefficient for downward vapor flow could be expressed as $Nu = x(1 + \frac{0.276}{x^4 Fr S})Re^{0.5}$, where $x = 0.9(1 + \frac{1}{S(\rho_l \mu_l / \rho_v \mu_v)^{0.5}})$. Furthermore, the numerical predictions of the heat transfer coefficients generated using this expression were shown to be in good agreement with the experimental results. In a later study, Rose [5] considered the effect of the pressure gradient on forced convection laminar film condensation on a horizontal tube. Two significant findings were reported, namely (a) the pressure

* Corresponding author. Tel.: +886 6 2757575x62140; fax: +886 6 2342081.
E-mail addresses: th0003@ms.twcat.edu.tw (H.-P. Hu), ckchen@mail.ncku.edu.tw (C.-K. Chen).
[1] Tel./fax: +886 6 2432495.

0017-9310/$ - see front matter © 2005 Elsevier Ltd. All rights reserved.
doi:10.1016/j.ijheatmasstransfer.2005.08.018

Nomenclature

C_p	specific heat of condensate at constant pressure (J/kg K)
d_e	equivalent circular diameter of elliptical tube (Eq. (23))
f	friction coefficient
$\bar{f}$	average friction coefficient
F	condensation parameter, $2/(SFr)$
Fr	Froude number, $u_\infty^2/g(d_e/2)$
Gr	Grashof number, $\frac{g(d_e/2)^3}{\nu_l^2}\frac{\rho_l-\rho_v}{\rho_l}$
g	acceleration due to gravity (m/s^2)
h_{fg}	latent heat (J/kg)
k	thermal conductivity (W/m K)
L	tube length (m)
L^+	dimensionless tube length, $2L/(d_e \tan\phi)$
Nu_R	local Nusselt number
Nu	local peripherally average Nusselt number
Nu_m	mean Nusselt number for whole tube surface
n	constant (0.805)
P	interfacial shear parameter, $\frac{\rho_v}{\rho_l}(\frac{\nu_l}{\nu_v})^{n-1}Gr^{1.4/6}$
Pr	Prandtl number
R	equivalent circular radius of elliptical tube, $d_e/2$
R_x^+	shear radius, $d_e u_x^*/(2\nu_l)$
R_x^*	wall shear parameter, $R_x^+/Gr_{d_e/2}^{1/3}$
Re	Reynolds number
S	sub-cooling parameter, $C_p(T_s - T_w)/(h_{fg}Pr)$
St	Stanton number, $Nu/(RePr)$
T	temperature (K)
T^+	dimensionless temperature, $(T - T_w)/(T_s - T_w)$
u_∞	vapor velocity of free stream (m/s)
u	condensate velocity (m/s)
u_x^*	shear velocity in x-direction, $\sqrt{\tau_{wx}/\rho}$
u_z^*	shear velocity in z-direction, $\sqrt{\tau_{wz}/\rho}$
u_x^+	dimensionless velocity, u_x/u_x^*
x	peripheral coordinate (m)
y	coordinate measured distance normal to surface (m)
y^+	dimensionless distance, yu_x^*/ν_l
Z	axial coordinate (m)
Z^+	dimensional axial coordinate, $2z/(d_e \tan\varphi)$

Greek symbols

δ	condensate film thickness (m)
δ^+	dimensionless film thickness, $\delta u_x^*/\nu_l$
φ	tube inclination angle with the horizontal
ν	kinematic viscosity (m^2/s)
ρ	density (kg/m^3)
τ	shear stress (N/m^2)
$\tau_{\delta x}$	interfacial vapor shear in x-direction
$\tau_{\delta z}$	interfacial vapor shear in z-direction
τ_{wx}	wall shear in x-direction
τ_{wz}	wall shear in z-direction
θ	angle measured from top of tube
ϕ	angle between the tangent to tube surface and the normal to direction of gravity
ε_m	eddy diffusivity for momentum
ε_h	eddy diffusivity for energy

Subscripts

l	liquid
e	edge of vapor boundary layer
s	saturation
v	vapor
w	tube wall
x	x-direction
z	z-direction
δ	vapor–liquid interface

gradient gives rise to an increase in the heat transfer coefficient over the forward part of the tube, particularly at higher values of $\frac{\rho_v h_{fg} v}{\Delta TK}$, and (b) the pressure gradient promotes an instability in the condensation film at certain locations over the rear half of the tube when $\frac{\rho_l g d}{8\rho_v u_\infty^2} < 1$.

Sarma et al. [6] investigated turbulent film condensation on a horizontal tube with isothermal wall conditions under an external flow of pure vapor. The interfacial shear was solved by means of the Colburn analogy. The numerical results were found to be in good agreement with the experimental data.

The studies presented above involved condensation on tubes with circular cross-sections. However, it is reasonable to assume that an elliptical tube whose major axis is aligned with the direction of gravity should also provide some of the advantages described above. For the case of free-convection film condensation on a horizontal tube, Cheng and Tao [7] found that the heat transfer coefficient performance of a horizontal elliptical tube is superior to that of a circular tube with the same condensation surface area. Meanwhile, for free and forced convection film condensation on a horizontal elliptic tube, Yang and Hsu [8] determined that for values of eccentricity in the range $e = 0.8$–8.95, the mean heat transfer was enhanced by approximately 16% at high values of F (low vapor flow velocity) and by 11% at low values of F compared to the case of a circular tube with an equal condensation surface area. Memory et al. [9] applied a Nusselt type analysis to the condition of free convection and revealed that an elliptical tube yielded an improvement of almost 11% in the heat transfer coefficient compared to a circular tube. For the case of forced convection, the interfacial shear was estimated in two ways: firstly, by using an asymptotic value of the shear stress under conditions of an infinite condensation rate, and secondly by

simultaneously solving the two-phase vapor boundary layer equations. For forced convection with the same approach velocity as for a circular tube, the elliptical tube provided a 2% decrease in the mean heat transfer coefficient results. Asbik et al. [10] predicted the onset of boundary layer transition in film condensation on a horizontal elliptical tube. Both the inertia and the convection terms were retained in the analysis. The work of Asbik et al. can be extended such that the beginning and the end of boundary layer transition can be determined.

Several researchers have focused on the problem of condensation on inclined tubes. For example, Hasson and Jakob [11] investigated the laminar film condensation of pure saturated vapor on inclined cylinders. Meanwhile, Mosaad [12] investigated combined free and forced convection laminar film condensation on an inclined circular tube with an isothermal surface, and demonstrated the effect of vapor velocity and gravity forces on the local Nusselt numbers. For the case of a tube of infinite length, it was shown that $Nu/(Re\cos\varphi)^{0.5} = \frac{0.9+0.728F^{0.5}}{(1+3.44F^{0.5}+F)^{0.25}}$. In a later study, Mosaad [13] considered the case of mixed-convection laminar film condensation on an inclined elliptical tube. The results indicated that the heat transfer performance of the inclined elliptical tube was superior to that of an inclined circular tube of equivalent diameter, and that the degree of enhancement increased with the degree of eccentricity.

Laminar film condensation has been widely discussed in the published literature. However, it is also worthwhile developing an understanding of turbulent flow condensation. According to Michael et al. [14], condensate films may be partially turbulent at high vapor velocities. Sarma et al. [6] assumed that condensate film flow takes place under a turbulent regime in regions located away from the upper stagnation point. Their study performed theoretical research into turbulent film condensation on a horizontal tube, and estimated the interfacial shear at the interface by applying the Colburn analogy. It was found that the numerical results were in good agreement with the experimental data. However, other than the research of Sarma et al. there has been relatively little recent investigation of the issues relating to turbulent film condensation on inclined elliptical tubes. Therefore, the aim of this study is to investigate turbulent film condensation on an isothermal inclined elliptical tube in terms of the local condensate film thickness and the heat transfer characteristics. The results developed in the current study are compare with those generated by previous theoretical results for turbulent film condensation.

2. Description of physical model

Consider an inclined elliptical tube immersed in a downward flowing pure vapor. The saturation temperature of the vapor is given by T_{sat}, the vapor is considered to move at a uniform velocity, u_∞, and the wall has a uniform temperature of T_w. Condensation occurs on the wall of the tube, and a continuous film of liquid runs downward over the tube in both the axial and peripheral directions. The physical model and the coordinate system adopted in the present study are shown in Fig. 1. The governing equations for the turbulent condensate film are described as follows:

Energy equation:

$$\frac{d}{dy}\left[\left(1+\frac{\varepsilon_h}{v_l}Pr\right)\frac{dT}{dy}\right]=0 \tag{1}$$

Thermal energy balance equation:

$$\frac{d}{dx}\int_0^\delta \rho_l u_x\,dy+\frac{d}{dz}\int_0^\delta \rho_l u_z\,dy=\frac{k_l}{h_{fg}}\frac{dT}{dy}\bigg|_{y=0} \tag{2}$$

Force balance equation in axial direction:

$$\rho(v+\varepsilon_m)\frac{du_z}{dy}\bigg|_{y=0}=\tau_{\delta z}+g\delta(\rho_l-\rho_v)\sin\varphi \tag{3}$$

Force balance equation in peripheral direction:

$$\rho(v+\varepsilon_m)\frac{du_x}{dy}\bigg|_{y=0}=\tau_{\delta x}+g\delta(\rho_l-\rho_v)\sin\phi\cos\varphi \tag{4}$$

where the wall shear stress

$$\tau_w=\rho(v+\varepsilon_m)\frac{du}{dy}\bigg|_{y=0} \tag{5}$$

The boundary conditions are given by:

$$\begin{aligned}&(1)\quad \text{at } y=0;\quad T=T_w\\&(2)\quad \text{at } y=\delta;\quad T=T_s\end{aligned} \tag{6}$$

These governing equations are subject to the following assumptions:

(1) The turbulent region is far larger than the laminar region and hence the laminar region can be neglected.
(2) The turbulent conduction term across the condensate layer is more significant than the convective term and hence the convective term can be neglected.
(3) The viscosity component and the sinking effect are more significant than the inertia force.
(4) Vapor boundary layer separation can be neglected.

Because of $\delta \ll (d_e/2)$, using the correlation equation of a vertical plate to analogize the heat transfer on axial direction of tube is quite reasonable [15]:

$$Nu_z=C_1Re_z^{0.8}Pr^{1/3} \tag{7}$$

In the turbulent region, the semi-empirical equations describe heat transfer in the flow around to the tube reported that [16]:

$$Nu_D=C_2Re_D^{0.8}Pr^{1/3} \tag{8}$$

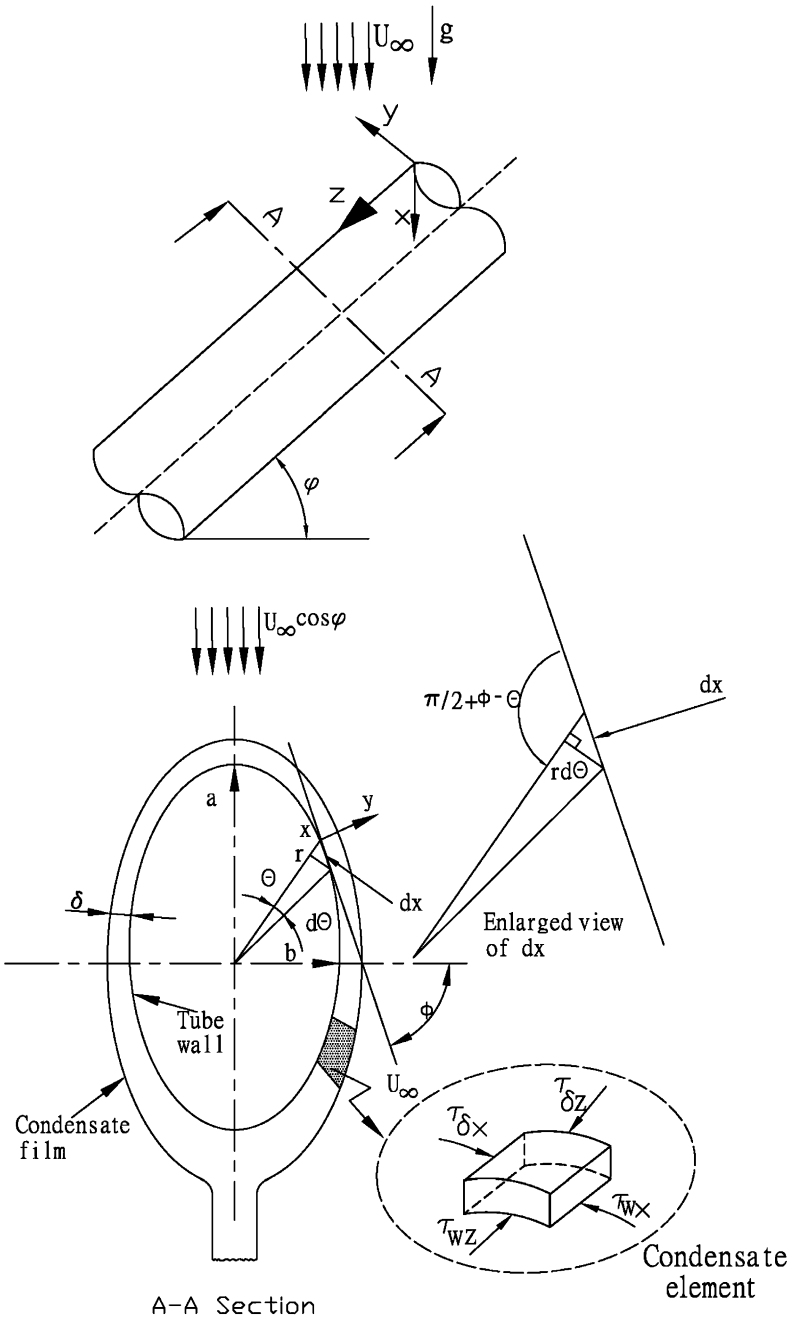

Fig. 1. Physical model and coordinate system.

According to the Colburn analogy, the heat transfer factor can be represented as:

$$\frac{\bar{f}}{2} = StPr^{2/3} \tag{9}$$

Combining Eqs. (7)–(9) gives:

$$f_z = 2C_1 Re_z^{n-1} \tag{10}$$

$$f_\theta = C_2 \pi Re_D^{n-1} \sin\theta \tag{11}$$

where the value of C_1 is 0.034, C_2 is 0.0266, and n is 0.805. Meanwhile:

$$Re_z = \frac{u_\infty z}{v_v}, \quad Re_D = \frac{u_\infty d_e}{v_v}, \quad St = \frac{Nu}{RePr}$$

The local shear stress is defined by the following relationship:

$$\tau_\delta = \tfrac{1}{2}\rho_v u_v^2 f \tag{12}$$

According to potential flow theory, the vapor velocity at the edge of the boundary is given by:

$$u_{ex} = u_\infty(1 + \sqrt{(1-e^2)})\cos\varphi\sin\phi \tag{13}$$

$$u_{ez} = u_\infty \sin\varphi \tag{14}$$

Combining Eqs. (10)–(14), it can be shown that the interfacial vapor shear in the z- and x-directions is given, respectively, by:

$$\tau_{\delta z} = C_1 \rho_v u_\infty^2 \sin^2\varphi Re_z^{n-1} = C_1 \rho_v u_\infty^2 \sin^2\varphi Re_D^{n-1} \left(\frac{z}{2R}\right)^{n-1} \quad (15)$$

$$\tau_{\delta x} = \tfrac{1}{2} u_\infty^2 (1+\sqrt{(1-e^2)})^2 C_2 \pi \rho_v Re_v^{n-1} \sin^3\phi \cos^2\varphi \quad (16)$$

Introducing Eqs. (15) and (16) into the forced balance equations (Eqs. (3) and (4)) yields the following equations:

$$\tau_{wz} = 2^{1-n} C_1 \rho_v u_\infty^2 \sin^2\varphi Re_z^{n-1} + g\delta(\rho_l - \rho_v)\sin\varphi \quad (17)$$

$$\tau_{wx} = \tfrac{1}{2} u_\infty^2 (1+\sqrt{(1-e^2)})^2 C_2 \pi \rho_v Re_D^{n-1} \cos^2\varphi \sin^3\phi + g\delta(\rho_l - \rho_v)\sin\phi\cos\varphi \quad (18)$$

The following dimensionless variables and equations are defined:

$$u_x^* = \sqrt{\tau_{wx}/\rho_l}, \quad u_z^* = \sqrt{\tau_{wz}/\rho_l}, \quad u_x^+ = \frac{u_x}{u_x^*},$$
$$u_z^+ = \frac{u_z}{u_z^*}, \quad T^+ = \frac{T - T_w}{T_s - T_w}, \quad y^+ = \frac{y u_x^*}{\nu_l},$$
$$R^* = \frac{R_x^+}{Gr_{d_e/2}^{1/3}}, \quad R_x^+ = \frac{d_e u_x^*}{2\nu_l}, \quad R_z^+ = \frac{d_e u_z^*}{2\nu_l}, \quad (19)$$
$$\delta^+ = \frac{\delta u_x^*}{\nu_l}, \quad Fr = \frac{u_\infty^2}{g(d_e/2)}, \quad Gr = \frac{g(d_e/2)^3}{\nu_l^2}\frac{\rho_l - \rho_v}{\rho_l}$$

The energy equation yields the following dimensionless energy equation:

$$\frac{d}{dy^+}\left[\left(1 + \frac{\varepsilon_m}{\nu_l} Pr\right)\frac{dT^+}{dy^+}\right] = 0 \quad (20)$$

The dimensionless boundary conditions of Eq. (20) are:

$$\begin{aligned} &(1) \quad \text{at } y^+ = 0; \quad T^+ = 0 \\ &(2) \quad \text{at } y^+ = \delta^+; \quad T^+ = 1 \end{aligned} \quad (21)$$

According to Yang and Hsu [8], the differential arc length can be expressed by the following equation:

$$dx = \frac{d_e}{2I(\phi)d\phi} \quad (22)$$

where

$$d_e = \frac{2a}{\pi}(1-e^2)\int_0^\pi (1 - e^2\sin^2\phi)^{-3/2} d\phi \quad (23)$$

$$I(\phi) = \pi(1-e^2\sin^2\phi)^{-3/2} \Big/ \int_0^\pi (1-e^2\sin^2\phi)^{-3/2} d\phi \quad (24)$$

where d_e is an equivalent diameter based on equal outside surface area, which is comparison with circular tubes.

Furthermore, the thermal energy balance equation (Eq. (2)) and the force balance equations (Eqs. (17) and (18)) can be rewritten in dimensionless form as follows:

$$\frac{d}{I(\phi)d\phi}\int_0^{\delta^+}\int_0^{y^+} \frac{\cos\varphi}{1+\frac{\varepsilon_m}{\nu}} dy^+ dy^+ + \frac{d}{dz^+}\int_0^{\delta^+}\int_0^{y^+} \frac{\sin\varphi}{1+\frac{\varepsilon_m}{\nu}} dy^+ dy^+ = SGr^{1/3} R_x^* \left.\frac{dT^+}{dy^+}\right|_{y^+=0} \quad (25)$$

$$\tan^2\varphi R_x^{*3} = R_x^* \left\{ C_1 \frac{\rho_v}{\rho_l}\left(\frac{\nu_l}{\nu_v}\right)^{n-1} Gr^{\frac{3n-1}{6}} \right\} \times Fr^{\frac{n+1}{2}} \sin^2\varphi (\tan\varphi Z^+)^{n-1} + \delta^+ \sin\varphi \quad (26)$$

$$R_x^{*3} = \frac{(1+\sqrt{1-e^2})^2}{4} R_x^* \left\{ 2^n \pi C_2 \frac{\rho_v}{\rho_l}\left(\frac{\nu_l}{\nu_v}\right)^{n-1} Gr^{\frac{3n-1}{6}} \right\} \times Fr^{\frac{n+1}{2}} \cos^2\varphi \sin^3\phi + \delta^+ \cos\varphi \sin\phi \quad (27)$$

where the sub-cooling parameter is given by $S = \frac{C_p(T_s - T_w)}{h_{fg} Pr}$.

The interfacial shear parameter is expressed by $p = \frac{\rho_v}{\rho_l}\left(\frac{\nu_l}{\nu_v}\right)^{n-1} Gr^{1.4/6}$.

The integration terms of Eq. (25) can be attained by modifying the expression of turbulent film condensation [6]:

$$u_x^+ = \int_0^{y^+} \frac{1}{1+\frac{\varepsilon_m}{\nu}} \cos\varphi \, dy^+ \quad (28)$$

$$u_z^+ = \int_0^{y^+} \frac{1}{1+\frac{\varepsilon_m}{\nu}} \sin\varphi \, dy^+ \quad (29)$$

The boundary condition is:

$$u^+ = 0 \quad \text{at } y^+ = 0 \quad (30)$$

The eddy diffusivity distribution presented by Kato et al. [17] is expressed by:

$$\frac{\varepsilon_m}{\nu} = 0.4y^+[1 - \exp(-0.0017y^{+2})] \quad (31)$$

Considering the condensation heat transfer, the heat transfer coefficient is given by:

$$K_l \left.\frac{\partial T}{\partial y}\right|_{y=0} = h(T_s - T_w) \quad (32)$$

Obviously, the local Nusselt number can be expressed as:

$$\frac{Nu_R}{Re_l^{1/2}} = \frac{Gr^{1/12}}{Fr^{1/4}} R_x^* \left.\frac{dT^+}{dy^+}\right|_{y^+=0} \quad (33)$$

where

$$Nu = \frac{hR}{k_l}, \quad Re_l = \frac{u_\infty d_e}{2\nu_l}$$

The local periphery mean Nusselt number is derived from:

$$\frac{Nu}{Re_l^{1/2}} = \frac{1}{\pi}\int_0^{\delta^+} \frac{Nu_R}{Re^{1/2}} d\theta \quad (34)$$

The overall mean Nusselt number for the entire surface of the tube can be written as:

$$\frac{Nu_m}{Re_l^{1/2}} = \frac{1}{L^+\pi}\int_0^{L^+}\int_0^{\delta^+} \frac{Nu_R}{Re^{1/2}} d\phi \, dZ^+ \quad (35)$$

3. Numerical method

The dimensionless governing Eqs. (20), (25), (26) and (27), subject to the relevant boundary conditions given in Eqs. (21) and (30), can be used to estimate δ^+, Re_Γ, R_x^* and Nu for the film condensation by means of the following procedure:

(1) Boundary conditions corresponding to the system conditions are input, i.e. at $i=0$, $j=0$, the dimensionless film thickness, δ^+, is zero. At the next node in the ϕ direction, i.e. $i=i+1$, the value of ϕ is given by $\phi_{i+1}=\phi_i+\Delta\phi$, where $\Delta\phi=(\pi/360)$. Similarly at the next node in the Z^+ direction, i.e. $j=j+1$, the value of z^+ is given by $z^+_{j+1}=z^+_j+\Delta z^+$, and $\Delta z^+=(L^+/100)$.

(2) Computation continues until the convergence criterion is attained, i.e.

$$\left|\frac{\delta_{i,j}^{+k+1}-\delta_{i,j}^{+k}}{\delta_{i,j}^{+k+1}}\right|\leqslant 1\times 10^{-6}$$

(3) This process is repeated at the next node position, and then subsequently at all nodes within the range, i.e. $0<\phi\leqslant\pi$, $0<z^+\leqslant L^+$.

(4) The local Nusselt number (Eq. (33)), Peripherally average local Nusselt number along the tube (Eq. (34)) and the overall mean Nusselt number (Eq. (35)) are then calculated.

4. Results and discussion

Fig. 2 presents the variation of the condensate dimensionless film thickness on an inclined elliptical tube with finite length. The domain factors include the forced-convection turbulent film condensation under a high vapor velocity, the interfacial shear force, the wall shear force, and the body force. The figure clearly demonstrates that the dimensionless film thickness increases as the dimensionless axial coordinate Z^+ increases. Specifically, the film thickness increases continuously from a minimum value at the upper stagnation point ($\phi=0$) as the value of ϕ increases. It can be seen that the film thickness reaches its maximum value in the downstream region of the tube at the lower stagnation point ($\phi=\pi$).

Fig. 3 presents the variation of the local Nusselt number of the condensate around the overall circumference of the tube, as calculated by Eq. (33). Regarding the variation of the heat transfer around the ellipse periphery, i.e. in the x-directional variation, it can be seen that the value of the shear Reynolds (R^*) number gradually increases with increasing angular position from its minimum value at the upper stagnation point to its maximum value at $\phi=\pi/2$. Subsequently, the value of the shear Reynolds number decreases gradually as the angular position is further increased, and reaches its minimum value at the lower stagnation point. These results are in full accordance with those predicted by potential flow theory, which states that the maximum value of the shear Reynolds number will occur at $\phi=\pi/2$. It is also noted that good agreement exists between the present results for the local Nusselt number and the theoretical results. Regarding the variation of the heat transfer in the Z^+ direction, it is observed that the dimensionless temperature gradient decreases as the condensate film flows towards the downstream region of the tube. Table 1 summarizes the angular positions of the maximum local heat transfer and the value of the heat transfer value at various points along the length of the inclined tube.

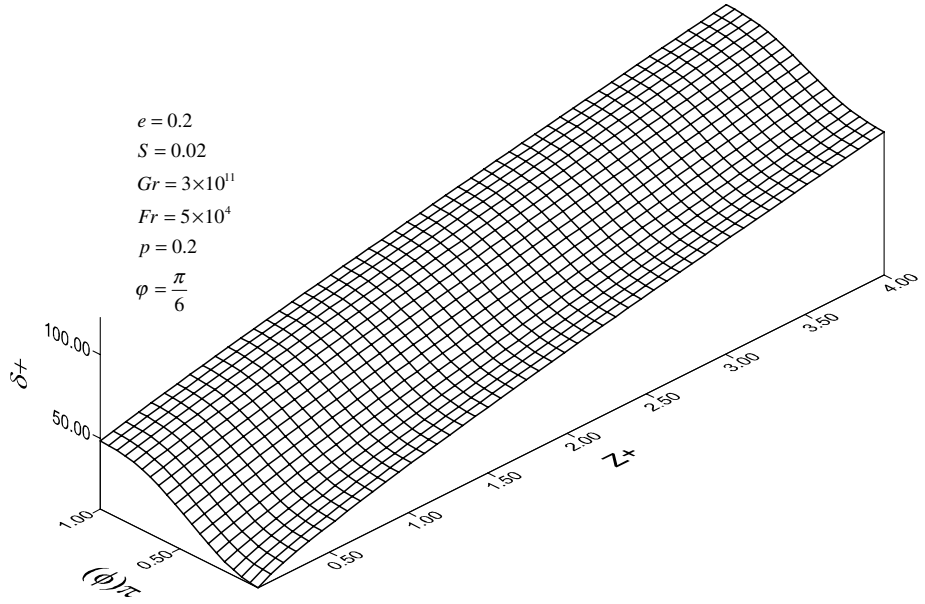

Fig. 2. Local film thickness on entire elliptical tube surface.

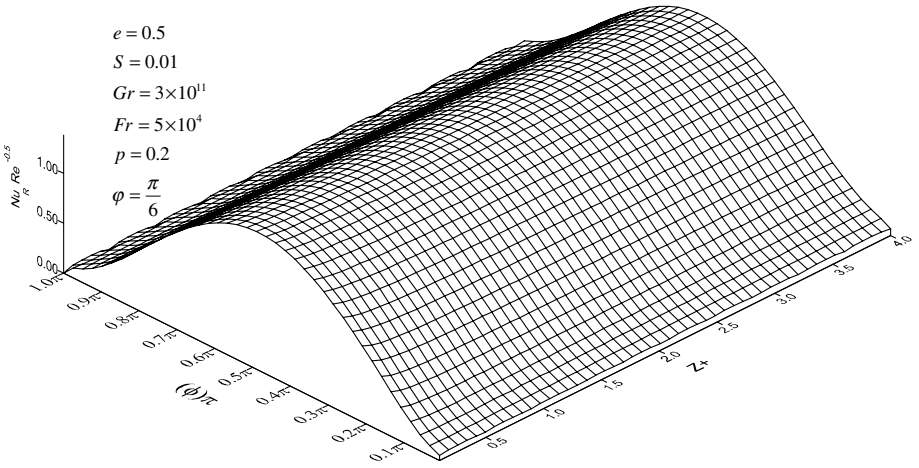

Fig. 3. Local Nusselt number on entire elliptical tube surface.

Table 1
Maximum value of local heat transfer coefficient

	Z^+								
	0.1	0.5	1	1.5	2.0	2.5	3.0	3.5	4.0
Angle of maximum heat transfer (ϕ)	177.8°	177.8°	182.1°	180°	180°	180°	180°	180°	180°
Heat transfer ($Nu/Re^{-0.5}$)	1.382	1.344	1.32	1.306	1.296	1.288	1.281	1.274	1.27

For three different sub-cooling parameter values, Fig. 4 plots the variation of the peripherally averaged local Nusselt number ($Nu(Re\cos\varphi)^{-0.5}$) along the inclined elliptical tube (Z^+), as calculated by Eq. (34). It is seen that for a constant value of Z^+, the peripherally averaged Nusselt number increases as the sub-cooling parameter value decreases. Besides, for a constant sub-cooling parameter value, the Nusselt number decreases as Z^+ increases from the upstream region of the tube towards the downstream region. Because of the influence of S on averaged Nusselt number is non-linear, the variation rate of averaged Nusselt number is larger when S are 0.002–0.004, and the influence on peripherally averaged local Nusselt number becomes less when S are 0.004–0.006. For a large distance from the upper tube end, the condensate film becomes fully developed, i.e., independent of Z. Hence, at $Z = 3$ where the peripherally averaged local Nusselt number for $S = 0.004$ and 0.006 are almost the same.

Fig. 5 presents the relationship between the peripherally averaged local heat transfer coefficient of the inclined tube and the dimensionless axial coordinate parameter, Z^+, for

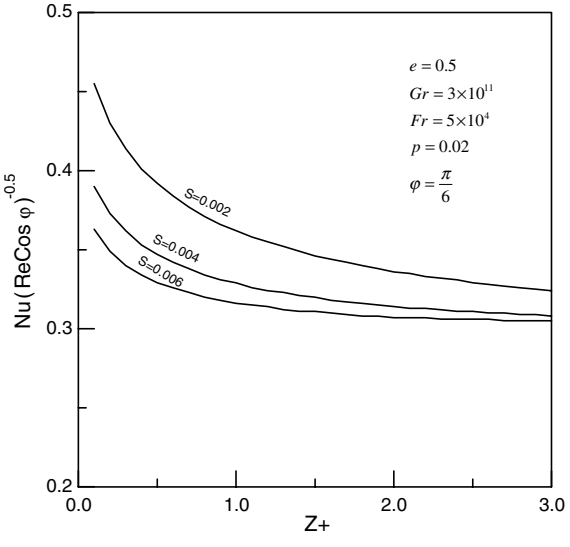

Fig. 4. Peripherally average local Nusselt number along the tube.

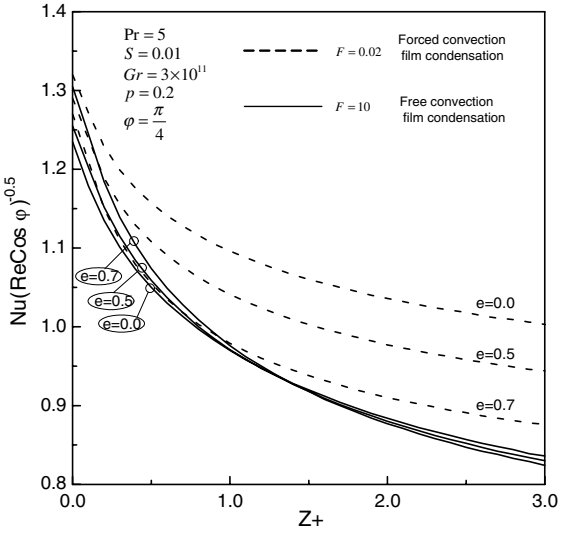

Fig. 5. Variation of peripherally average local Nusselt number along the tube.

eccentricity values of $e = 0.0$, 0.5 and 0.7. The figure presents the results for both the forced and the free-convection film condensation cases. Considering the turbulent film condensation under a lower vapor velocity ($F = 10$), a higher eccentricity increases the heat transfer prior to the halfway point along the tube length, but decreases the heat transfer thereafter. Meanwhile, for turbulent film condensation under a high vapor velocity ($F = 0.02$), the velocity and the shear force are the dominating factors, and therefore increasing the eccentricity decreases the vapor velocity around the tube, with the result that the heat transfer coefficient is reduced.

Fig. 6 shows the variation in the overall mean Nusselt number with the elliptical tube inclination angle for seven different values of eccentricity. Under a high vapor velocity, reducing the eccentricity tends to increase the overall mean Nusselt number. Furthermore, the figure shows that the Nusselt number has its maximum value when the inclination angle of the maximum heat transfer (φ_{max}) occurs, and that the Nusselt number subsequently reduces as the inclination angle increases. The results of Fig. 6 permit the optimal inclination angle to be identified for elliptical tubes with different degrees of eccentricity.

Fig. 7 shows the variation of the mean Nusselt number with the elliptical tube inclination angle for various values of dimensionless tube length, L^+. It is observed that for a constant inclination angle, the mean Nusselt number decreases with increasing L^+. Hence, the results reveal that the optimum angle of inclination is a function of the dimensionless tube length.

Fig. 8 shows the variation of the mean Nusselt number with the vapor velocity for the particular case of an inclined elliptical tube with a zero inclination angle, i.e. $\varphi = 0$. The figure compares the present results with the theoretical data and experimental results presented in an earlier study [6,18]. It can be seen that there is a broad similarity between the two sets of results at both low and high vapor velocities. It is noted that in the high velocity regime ($F < 0.1$), the Nusselt number increases as the F value decreases. Significantly, the rate of increase of the coefficient with velocity is greater than that indicated by laminar theory. According to Lee et al. [19], this discrepancy may be due to the onset of turbulence in the condensate film in the high vapor velocity region. In the low velocity regime ($1 < F < 1000$), the mean Nusselt number is seen to increase as the F value increases. Fig. 8 confirms that there is a broad agreement between the two sets of data in both the low and the high vapor velocity regimes.

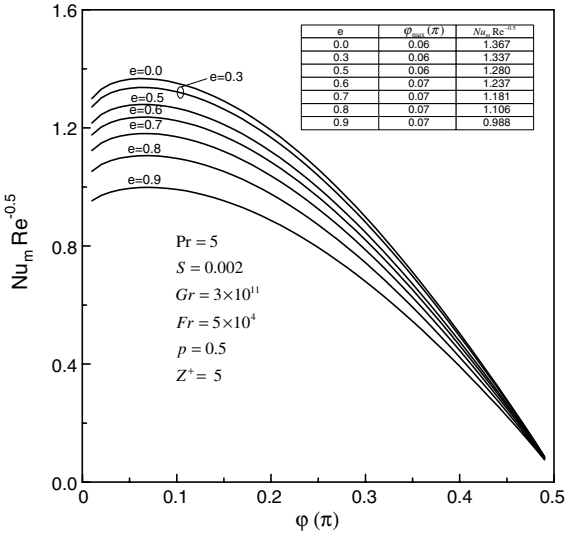

e	φ_{max} (π)	$Nu_m Re^{-0.5}$
0.0	0.06	1.367
0.3	0.06	1.337
0.5	0.06	1.280
0.6	0.07	1.237
0.7	0.07	1.181
0.8	0.07	1.106
0.9	0.07	0.988

Fig. 6. Variation of overall mean Nusselt number on inclination angle—effect of eccentricity.

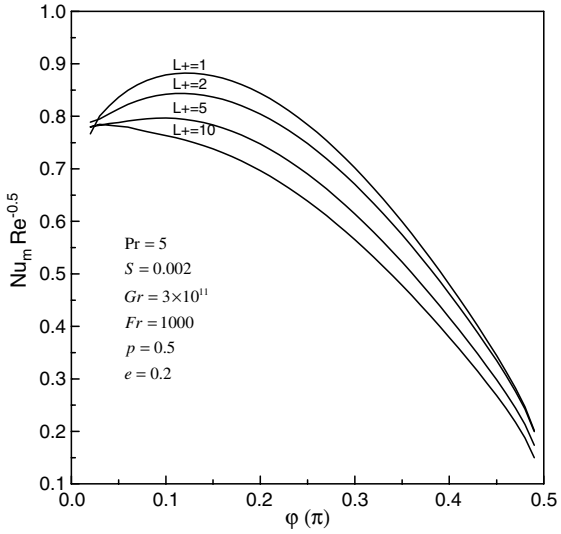

Fig. 7. Variation of overall mean Nusselt number on inclination angle—effect of L^+.

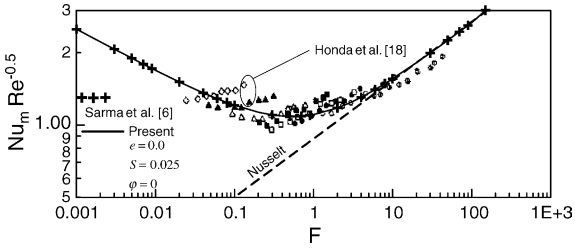

Fig. 8. Comparison of present results with theoretical and experimental data.

5. Concluding remarks

The following conclusions can be drawn from the results of the present theoretical study:

(1) For turbulent film condensation under lower vapor velocities, a higher eccentricity will increase the heat transfer over the upper half of the tube length, but will decrease the heat transfer over the lower half of the tube. Meanwhile, for turbulent film condensation under high vapor velocities, the velocity and shear force are the dominating factors. Therefore,

an increased eccentricity will reduce the heat transfer. Hence, when designing a heat exchanger, under the force convection turbulent condensation, we suggest applying a circular tube; however, under the free convection turbulent condensation, for increasing heat transfer coefficient, an elliptical tube is a better choice.

(2) The mean Nusselt number decreases as the dimensionless tube length, L^+, increases. The optimum angle of inclination of the elliptical tube varies both with the tube length and with the degree of eccentricity.

(3) For the case of a zero inclination angle, i.e. $\varphi = 0$, the overall mean Nusselt number increases as the F value increases in the low velocity flow regime ($1 < F < 1000$), but decreases with increasing F value in the high velocity regime ($F < 0.1$).

Acknowledgement

The current authors gratefully acknowledge the support provided to this project by the National Science Council of the Republic of China under Contract Number NSC-92-2218-E-165-002.

References

[1] E.M. Sparrow, J.L. Gregg, Laminar condensation heat transfer on a horizontal cylinder, ASME J. Heat Transfer 81 (1959) 13–18.

[2] V. Dhir, J. Lienhard, Laminar film condensation on plane and axisymmetric bodies in nonuniform gravity, ASME J. Heat Transfer 93 (1971) 97–100.

[3] I.G. Shekriladze, V.I. Gomelauri, Theoretical study of laminar film condensation of flowing vapor, Int. J. Heat Mass Transfer 9 (1966) 581–591.

[4] T. Fujii, H. Uehara, C. Kurata, Laminar filmwise condensation of flowing vapor on a horizontal condenser, Int. J. Heat Mass Transfer 15 (1972) 235–246.

[5] J.W. Rose, Effect of pressure gradient in forced convection film condensation on a horizontal tube, Int. J. Heat Mass Transfer 27 (1984) 39–47.

[6] P.K. Sarma, B. Vijayalakshmi, F. Mayinger, S. Kakac, Turbulent film condensation on a horizontal tube with external flow of pure vapors, Int. J. Heat Mass Transfer 41 (1998) 537–545.

[7] S. Cheng, J. Tao, Study of condensation heat transfer for elliptical pipes in a stationary saturated vapor, ASME J. Heat Transfer 96 (1988) 405–408.

[8] S.A. Yang, C.H. Hsu, Free- and forced-convection film condensation from a horizontal elliptical elliptic tube with a vertical plate and horizontal tube as special cases, Int. J. Heat Fluid Flow 18 (1997) 567–574.

[9] S.B. Memory, V.H. Adams, P.J. Marto, Free and forced convection laminar film condensation on horizontal elliptical tubes, Int. J. Heat Mass Transfer 40 (1997) 3395–3406.

[10] M. Asbik, H. Boushaba, R. Chayuane, B. Zeghmati, A. Khmou, Prediction of onset of boundary layer transition in film condensation on a horizontal elliptical cylinder, Numer. Heat Transfer, Part A 43 (2003) 83–109.

[11] K.E. Hasson, M. Jakob, Laminar film condensation of pure saturated vapor on inclined cylinders, ASME J. Heat Transfer 80 (1958) 887–897.

[12] M. Mosaad, Combined free and forced convection laminar film condensation on an inclined circular tube with isothermal surface, Int. J. Heat Mass Transfer 42 (1999) 4017–4025.

[13] M. Mosaad, Mixed convection laminar film condensation on an inclined elliptical tube, ASME J. Heat Transfer 123 (2001) 294–300.

[14] A.G. Michael, J.W. Rose, L.C. Daniels, Forced convection condensation on a horizontal tube—experiments with vertical downflow of steam, ASME J. Heat Transfer 111 (1989) 792–797.

[15] F.P. Incropera, D.P. DeWitt, Fundamentals of Heat and Mass Transfer, John Wiley, New York, 2002.

[16] J.P. Holman, Heat Transfer, McGraw-Hill, New York, 1968.

[17] H. Kato, N.N. Shiwaki, M. Hirota, On the turbulent heat transfer by free convection from a vertical plate, Int. J. Heat Mass Transfer 11 (1968) 1117–1125.

[18] H. Honda, S. Zozu, B. Uchima, T. Fujii, Effect of vapor velocity on film condensation of R-113 on horizontal tubes in across flow, Int. J. Heat Mass Transfer 29 (3) (1986) 429–438.

[19] W.C. Lee, S. Rahbar, J.W. Rose, Film condensation of refrigerant 113 and ethanediol on a horizontal tube—effect of vapor velocity, ASME J. Heat Transfer 106 (1984) 524–530.